



Universiteit
Leiden
The Netherlands

Chemokines in Ewing sarcoma

Sand, L.G.L.

Citation

Sand, L. G. L. (2016, October 27). *Chemokines in Ewing sarcoma*. Retrieved from <https://hdl.handle.net/1887/43794>

Version: Not Applicable (or Unknown)

License: [Licence agreement concerning inclusion of doctoral thesis in the Institutional Repository of the University of Leiden](#)

Downloaded from: <https://hdl.handle.net/1887/43794>

Note: To cite this publication please use the final published version (if applicable).

Cover Page



Universiteit Leiden



The handle <http://hdl.handle.net/1887/43794> holds various files of this Leiden University dissertation

Author: Sand, Laurens

Title: Chemokines in Ewing sarcoma

Issue Date: 2016-10-27

Chapter 7

Evaluation of CXCR4 specific endocytosis using an activatable peptide

**L.G.L. Sand, S. van der Wal, P.C.W. Hogendoorn, C.M. Korne, K. Szuhai, F.W.B. van
Leeuwen, T. Buckle**

In preparation

ABSTRACT

For many tumors the membrane-bound chemokine receptor CXCR4 is an important factor in tumor progression and metastasis. Upon binding of its dominant ligand CXCL12/stromal derived factor 1 (SDF-1), CXCR4 is internalized via endocytosis and degraded or recycled. To specifically study the endocytosis process, we have synthesized the receptor specific and redox sensitive/thiol-activatable Cy5-S-S-Cy3-Ac-TZ14011 peptide. In vitro analysis demonstrated that Foster Resonance Energy Transfer (FRET) with Cy5 quenched the Cy3 emission in the disulfide-containing label, while cleavage of this disulfide bond resulted in a fluorescently active Cy3-Ac-TZ14011 peptide. Real-time evaluation of receptor internalization in Ewing sarcoma cell lines demonstrated both a qualitative and quantitative increase in Cy3 intensity when CXCR4 was expressed at “high” levels. This method enables studying of CXCR4 dynamics at the live cell level and can discriminate between internalized and non-internalized receptors. This principle might be transferred to other receptor endocytosis studies.

KEYWORDS

FRET, internalization, fluorescence, sarcoma, chemokines, Ewing sarcoma

INTRODUCTION

CXCR4 is of major importance for a number of processes in the tumor microenvironment [1-3], for example in Ewing sarcoma (EWS), an aggressive, highly metastatic and well vascularized bone tumor [4]. It has been associated with the level of angiogenesis, metastasis and survival [5-9]. A complex network of regulation processes allows CXCR4 to perform its tumorigenic functions. One of these processes is the CXCR4 trafficking to and from the membrane and the availability on the membrane [10,11]. This process is cell/tissue-type dependent [10,12]. The general view is that newly synthesized CXCR4 receptors are directed towards the cell surface. Upon extracellular binding of its dominant ligand CXCL12 also known as stromal derived factor 1, the receptor then internalizes and is subsequently degraded by lysosomes or is recycled to the cell membrane [13]. The endocytosis process of CXCR4 is influenced by different tracks, including dynamin-dependent and clathrin-dependent endocytosis, lipid rafts or macropinocytosis [12,14,15].

To image CXCR4 *in vitro* and *in vivo* a variety of agents have been developed [16]. Especially fluorescent and hybrid (both fluorescent and radioactive) analogues of the antagonistic CXCR4 targeting peptide T140 showed great potential in flow cytometry, microscopy and non-invasive SPECT imaging [17-19]. However, these agents can only image and track CXCR4 and cannot on its own be used to discriminate between intracellular and extracellular CXCR4.

General the principle of an activatable peptide, a peptide active upon cleavage, has dominantly been used for enzymatic activity [20]. As an imaging agent this principle opens the possibility to use two tissue characteristics. For example, by combining a pH sensitive bond with a receptor targeting peptide, only in an acidic environment with the present receptor the signal after cleavage would appear [21]. This principle with an Iridium-Cy5 FRET pair for long luminescence lifetime has recently been reported [22].

When coupled to a receptor targeting agent, the activatable peptide principle can be also used to study the endocytosis dynamics and intracellular trafficking of receptors in live cells

when the receptor is internalized upon binding of the activatable peptide which is intracellularly cleaved [23]. Thereby, it can distinguish the internalized fraction of the studied receptor from the rest. To study the CXCR4 endocytosis dynamics we coupled an activatable Cy5-S-S-Cy3 label, to the CXCR4 binding and internalizing peptide Ac-TZ14011 [16,18,19]. Cy3 and Cy5 are a well-known Förster Resonance Energy Transfer (FRET) pair [24,25]. We reasoned that upon binding and cellular internalization of Cy5-S-S-Cy3-Ac-TZ14011, the disulfide bond between the two dyes will be reduced in the reducing intracellular environment. This will result in a change in fluorescence emitted by the peptide from 680 nm to 580 nm when excited at the 550 nm (**Figure 1**). This effect was studied in high and low CXCR4 RNA expressing EWS cell lines to validate the activatable CXCR4 targeting compound as receptor specific endocytosis tracer.

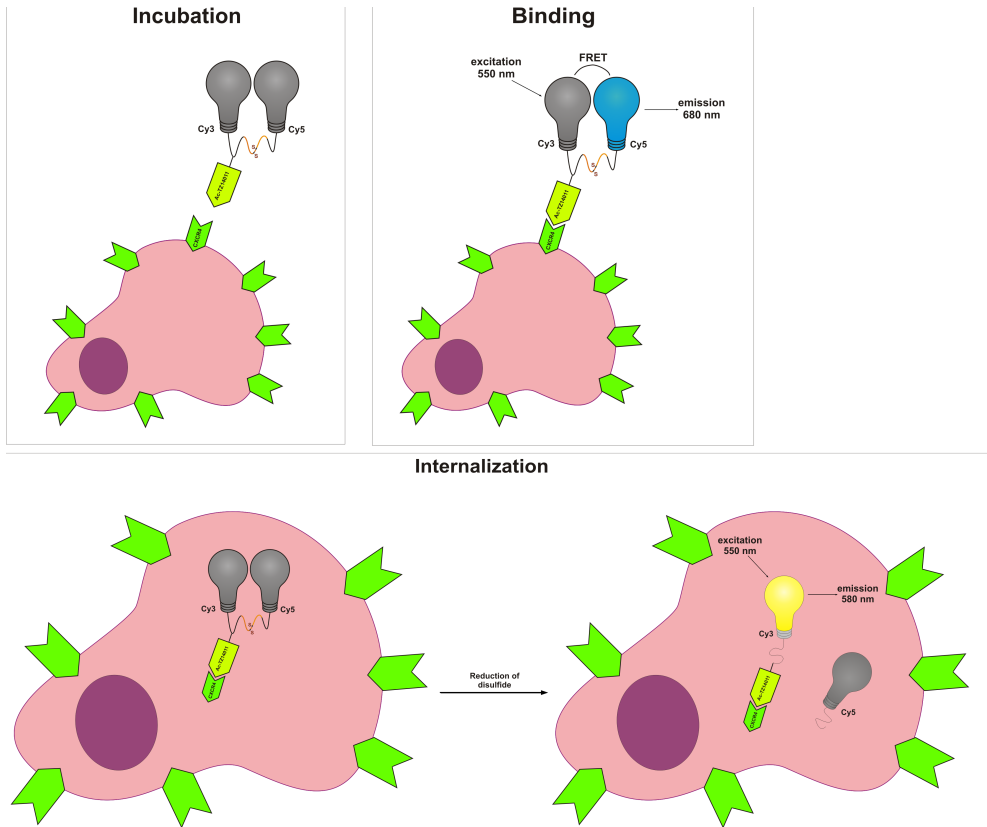


Figure 1: Principle of receptor targeted activatable imaging agents. The Cy3-Cy5 FRET label, with a disulfide bond between the dyes (depicted in orange), coupled to the CXCR4 targeting peptide Ac-TZ14011 is administrated to live cells. When the peptide (Cy5-S-S-Cy3-Ac-TZ14011) is excited at 550 nm the Cy3 transfers the energy to Cy5 which emits light of 680 nm. Upon binding, the Cy5-S-S-Cy3-Ac-TZ14011-CXCR4 complex is internalized and the disulfide bond between Cy3 and Cy5 is reduced in a reducing intracellular environment. When the reduced peptide is excited at 550 nm, Cy3 cannot transfer the energy to Cy5 and emits light at a wavelength of 580 nm.

MATERIAL & METHODS

Chemical synthesis, purification and characterization

All chemicals were obtained from commercial sources and used without further purification. Semi-preparative HPLC was performed on a Waters HPLC system using a 1525EF pump, a 2489 dual wavelength absorbance detector (Waters Chromatography, Etten-Leur, the Netherlands) and a flow rate of 6 mL/min using a gradient of 5 % to 95 % acetonitrile in water with 0.1 % TFA of 100 min (Dr. Maisch Reprosil-Pur C18-AQ, 10 μm (250 \times 10 mm) column) (Dr. Maisch High Performance LC, Ammerbuch-Entringen, Germany). Analytical HPLC was performed using a flow rate of 1 mL/min using a gradient of 5 % to 95 % acetonitrile in water with 0.1 % TFA of 40 min (Dr. Maisch Reprosil-Pur C18-AQ 5 μm , (250 \times 4.60 mm) column) (Dr. Maisch High Performance LC). A Waters Acquity UPLC-ESI-MS system using a Acquity UPLC photodiode array detector, an SQ Detector mass spectrometer and a flow rate of 0.5 mL/min (Waters BEH C18 130 \AA 1.7 μm (100 \times 2.1 mm) column) (all from Waters Chromatography) was used for ESI-MS analysis. MALDI-TOF analysis was performed on a Bruker Microflex (Bruker Daltonics, MA, US) using a matrix of α -cyano-4-hydroxycinnamic acid and a reference of Granuliberin R ($[\text{M}+\text{H}]^+ = 1423.7$ Da). Freeze-drying was performed by dissolution or dilution of the compound in *tert*-butanol/ H_2O (1:1 v/v) and freeze-drying in a Christ Alpha RVC equipped with a Mitsubishi VaCo 2 condenser (Christ, Osterode am Harz, Germany).

Synthesis of Boc-Cys(S-CH₂CH₂-NH₂)-OH (1)

Boc-Cys(Npys)-OH (187 mg, 0.5 mmol) (Sigma-Aldrich GmbH, Steinheim am Albuch, Germany), and cysteamine hydrochloride (45 mg, 0.4 mmol) were dissolved in THF/ H_2O (1:1 v/v, 5 mL). *N*-methyl morpholine (NMM, 20 μL , 0.2 mmol) was subsequently added and the reaction mixture was stirred overnight. Disappearance of the cysteamine starting material from the now orange reaction mixture was confirmed by TLC (10% MeOH/ CH_2Cl_2 , staining with ninhydrin) and ESI-MS indicated a mass of 297.1 Da, corresponding to the $[\text{M}+\text{H}]^+$ of the product (calculated mass 297.1 Da). In addition, two other masses corresponding to 3-nitro-2-pyridine thiol (156.8 Da) and excess Boc-Cys(Npys)-OH (375.9 Da) were also found. This crude material was used directly in the next synthesis.

Synthesis of Boc-Cys(S-CH₂CH₂-NH-Cy5)-OH (2)

To 0.5 mL of the reaction mixture of compound 1 (40 μmol), NMM (10 μL , 100 μmol) was added to adjust to pH to \sim 8. Cy5-OSu [26] (5 mg, 5.4 μmol) was added and stirred for 2.5 h. Hereafter the mixture was diluted with 4 mL H_2O and purified by semi-preparative HPLC (elution time: $t_R = 33$ min). The fraction containing the product was freeze-dried to yield a blue fluffy solid (0.8 mg, 0.7 μmol). MALDI-TOF: $[\text{M}]^+$ found 1043.96 Da, calculated 1043.29 Da. The Boc group was found to be partially removed during storage in the TFA buffer: mass $[\text{M}]^+$ found was 943.83 Da, calculated mass was 943.24 Da.

Synthesis of Cy3-Cys(S-CH₂-CH₂-NH-Cy5)-OH (Cy5-S-S-Cy3, 3)

The Boc-group was completely removed from compound 2 (0.4 mg, 0.35 μmol) by addition of trifluoroacetic acid (TFA, 1 mL) and stirring for 1 h. The TFA was removed by concentration *in vacuo* and the residue was co-evaporated with chloroform twice, after which it was lyophilized. The dry compound was dissolved in phosphate buffer (1 mL, 100 mM, pH 8.3), followed by the addition of Cy3-TFP ester [27] (3 mg, 3 μmol) in DMF (200

μL). The reaction mixture was allowed to stir for 3 h and was diluted with 4 mL H_2O . After acidification with 10 μL AcOH. The product was purified by semi-preparative HPLC ($t_R = 26$ min). This fraction was freeze-dried to yield a purplish blue fluffy solid (0.4 mg, 0.21 μmol) with an analytical HPLC $t_R = 23.9$ min. Mass $[\text{M}-\text{H}]^+$ found was 1664.46 Da, calculated mass was 1663.43 Da (**Figure S1**). Mass $[\text{M}-2\text{H}+\text{Na}]^+$ found was 1686.45 Da, calculated mass was 1685.41 Da. Some disulfide cleavage induced by the ionization process was also observed generating ions of 824.67 Da and 842.66 Da [28].

Synthesis of Cy3-Cys(S-CH₂-CH₂-NH-Cy5)-[Ac-TZ14011] (Cy-S-S-Cy3-Ac-TZ14011, 4)

Compound 3 (0.2 mg, 0.1 μmol), PyBOP (2 mg, 4 μmol), Ac-TZ14011 [29] (2 mg, 0.3 μmol) and NMM (10 μL , 100 μmol) were dissolved in DMF (400 μL) and stirred for 2 h, after which water was added and the reaction was allowed to continue for another 30 min. The reaction mixture was diluted with 4 ml water, acidified with AcOH (10 μL) and purified by semi-preparative HPLC ($t_R = 32$ min). The fraction containing the product was freeze-dried to yield a purplish blue fluffy solid that was dissolved in 1 mL water. The concentration was determined by spectroscopy using a molar extinction coefficient of 2.4×10^5 [30] and was found to be 2.4 μM . The resulting stock solution was used for all further experiments. MALDI-TOF Mass $[\text{M}]^+$ found a mass of 3752.36 Da, calculated mass was 3751.49 Da ($t_R = 26.1$ min on analytical HPLC) (**Figure S2**).

Photophysical properties of the Cy3-Cy5 FRET labelling

Compound 3 was dissolved in PBS (3 mL, 3 μM final volume and concentration) and absorbance was measured in a quartz cuvette on a Ultraspec 3000 (Amersham Pharmacia Biotech, Munich, Germany) subtracting a PBS blank. Fluorescence properties were analyzed on a Perkin-Elmer LS-55 spectrofluorometer (Perkin-Elmer, Waltham, MA, US). After excitation at 520 nm, the emission spectrum was obtained between 530-750 nm. A 2D excitation/emission scan was obtained while exciting between 450-750 nm with 5 nm increments with emission recorded at 450-750 nm for each scan. Results were incorporated into 2D and 3D representations using MatLab (Mathworks Inc., Massachusetts, USA) software using the surf(x,y,z) command. A DTT solution was subsequently added (50 mM stock, 60 μL) to the cuvette for a final concentration of 1 mM. After mixing, the cuvette was allowed to incubate for 140 min, after which fluorescence was measured every 5 min after excitation at 520 nm. When the compound was completely reduced, a 2D and 3D representation was recorded similar to the one described above.

Cell culture

EWS cell line TC32, having a high CXCR4 RNA expression, was obtained from the EuroBoNeT consortium collection (Institute of Pathology, University Medical Center, Düsseldorf, Germany) [31]; A673, having a low CXCR4 RNA expression, was obtained from the ATCC. TC32 and A673 were cultured in Iscove's modified Dulbecco's medium (IMDM) containing GlutaMAX supplement under standard culture conditions. Both media were supplemented with 1% streptomycin/penicillin and 10% heat-inactivated FCS (all were obtained from Life Technologies, Bleiswijk, The Netherlands).

Confocal imaging

Cells were plated on a glass bottom culture dish (MatTek corporation, Ashland, Ma, USA) 24 h before imaging to let the cells attach to the bottom. Hoechst 33258 and lysotracker DND-

26 (Life Technologies) were added at a final concentration of 1 $\mu\text{g}/\text{mL}$ for 1 h and excess was washed away prior to imaging. Cy-S-S-Cy3-Ac-TZ14011 was sonicated (1 min) and added to the dish at a final concentration of 4 μM and present in media during first 3 h of imaging. Live cell imaging was performed on SP8 with a white light laser and a UV laser by sequential imaging at the dye its optimal excitation wavelength and measured in their specific emission range at a 63 times magnification under standard culture conditions with a HC PL APO CS2 63x/1.40 OIL lens (Leica, Eindhoven, The Netherlands) (**Table 1**). Imaging was performed during 3 h. After 3 h imaging cells were washed incubated standard culture conditions to be measured at 24 h and 72 h.

Table 1: Excitation and emission wavelength ranges of the different fluorophores used during imaging

| Fluorophore | Excitation | Emission detection range |
|-------------|-------------------|--------------------------|
| Hoechst | 405 nm (UV diode) | 415-509 nm |
| DND-26 | 504 nm | 510-530 nm |
| Cy3 | 552 nm | 558-593 nm |
| Cy5 | 631 nm | 652-709 nm |
| FRET | 552 nm | 652-709 nm |

Image analysis

Quantitative fluorescence intensity levels of multiple images (minimal 3 per measurement) were obtained using LASX software by calculating the mean intensity of the cell covered area (Leica) and each image was background-corrected by the analyzed the fluorescence intensity levels of the nuclei present in the analyzed area (observed by Hoechst 33528 staining). As controls, images were made before adding Cy-S-S-Cy3-Ac-TZ14011 and after adding Ac-TZ14011-MSAP [17], which contains a Cy5 but no Cy3 fluorophore, was used as control for FRET fluorescence when exciting at 552 nm and measuring at 652-709 nm. All fluorescence images collected at different wavelengths are shown separately in **Figure S3 and S4**.

RESULTS

Synthesis and in vitro validation of activatable Cy-S-S-Cy3-Ac-TZ14011

As presented in **Figure 2**, the CXCR4 endocytosis tracer is generated by linking the synthesized Cy5-S-S-Cy3 FRET label to Ac-TZ14011 by using its carboxylic acid. FRET-label synthesis was started using Boc-Cys(Npys)-OH as a straightforward platform for a asymmetric disulfide bond (**Figure 2**, compound 1). Crude material 1 was used for conjugation with an activated ester of sulfonated Cy5 to afford compound 2. After purification of compound 2, the Boc protecting group was removed and the activated ester of sulfonated Cy3 was added under aqueous conditions yielding Cy5-S-S-Cy3 (3). Ultimately, conjugation of Cy5-S-S-Cy3 (3) with the targeting peptide Ac-TZ14011 yielded the activatable CXCR4 tracer Cy5-S-S-Cy3-Ac-TZ14011 (4).

The photophysical properties of compound 3 were analyzed *in vitro* by measuring the absorbance and FRET efficiency (**Figure 3 and S3A**). The absorbance demonstrated a pattern matching the Cy3 and Cy5 absorbance peaks. As a result of a difference in their extinction coefficients, the Cy5 signal intensity was higher than that of the Cy3 signal. The FRET efficiency was assayed in PBS and showed low Cy3 fluorescence upon excitation at 520 nm but a high

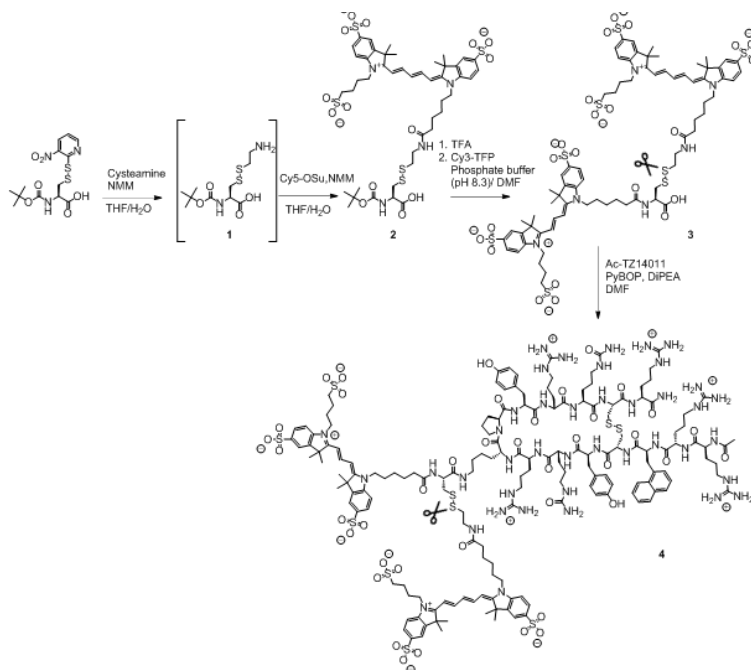


Figure 2: Synthesis of Cy-S-S-Cy3-Ac-TZ14011.

Synthesis was started with Boc-Cys(Npys)-OH which contains a disulfide bond. This is transformed to compound 1 with an asymmetrical disulfide bond as result and compound 1 is subsequently coupled to sulfonated Cy5, resulting in compound 2. By adding Cy3-TFP, Cy3 can be linked to generate compound 3, the Cy3-Cy5 FRET dimer. Ac-TZ14011 is coupled to compound 3 at the carboxylic acid group to generate compound 4, the CXCR4 endocytosis peptide (Cy5-S-S-Cy3-Ac-TZ14011). The scissors appoint the cleavage site.

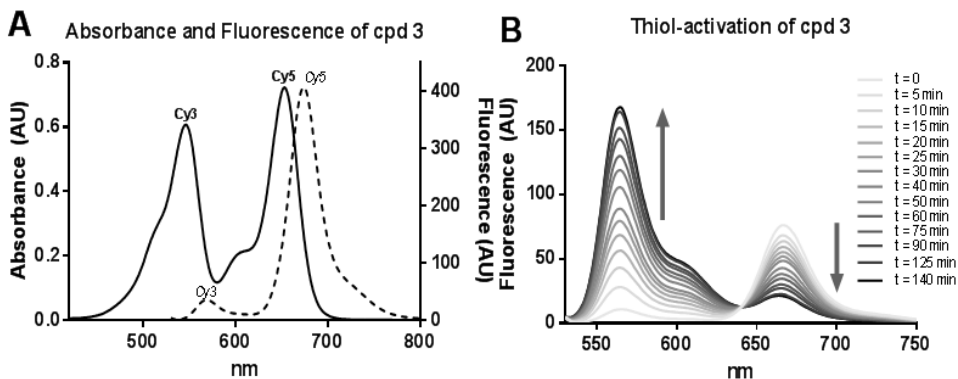


Figure 3: Photophysical properties of the Cy3-Cy5 FRET labelling. A) Absorbance and fluorescence spectra of compound 3 (3 μ M in PBS) in solid line, with the fluorescence spectrum upon excitation of Cy3 at 520 nm depicted in dotted line. B) Fluorescence spectra of the time-dependent disulfide reduction of 3 with DTT at various time points upon excitation at 520 nm. Increase in Cy3 fluorescence at 570 nm was found to be 20-fold, demonstrating *in vitro* functionality of compound 3.

Cy5 fluorescence (Figure 3A and S3A).

To test the cleavage of the FRET-pair and thereby the reactivation of the Cy3 signal, the strong disulfide reducing agent dithiothreitol (DTT) was used. Fluorescence spectrometric analysis during 140min (Figure 3B) revealed a gradual reduction in Cy5 fluorescence and increase in Cy3 fluorescence; after 140 min a 20-fold increase in Cy3-fluorescence was obtained. This suggests a \sim 95% FRET efficiency of compound 3 (Figure S5). Cy-S-S-Cy3-Ac-TZ14011 (4) was also examined by fluorescence spectroscopy prior to- and after DTT reduction. Herein a threefold increase in Cy3 fluorescence was observed between non-reduced and reduced state (data not shown).

***In vitro* validation of Cy-S-S-Cy3-Ac-TZ14011 by measuring CXCR4 endocytosis in EWS cell lines**

Further *in vitro* validation of Cy-S-S-Cy3-Ac-TZ14011 was performed using EWS cell lines TC32 and A673. Directly after Cy-S-S-Cy3-Ac-TZ14011 administration, a staining was observed which was consistent with previous observations; a strong cell membrane staining in TC32 and some membrane staining in A673 (**Figure S3A and S4A**). After 1 h, in both cell lines, a clustered staining which partly overlapped with the lysosome tracker DND-26 staining. Over time the Cy5 and FRET fluorescence signal decreased in both cell lines and only TC32 demonstrated an overall increase in Cy3 fluorescence signal (**Figure S3 and S4**). No clear membrane staining of the Cy3 signal like the Cy5 signal has been observed in both cell lines.

Quantitative analysis of the mean fluorescence intensity demonstrated similar trends; in both cell lines a decreasing trend in Cy5 and FRET signal was observed and in TC32 an increasing trend of Cy3 signal was observed which was significant after 72 h ($P < 0.03$) (**Figure 4**). In A673 no trend in Cy3 signal was observed.

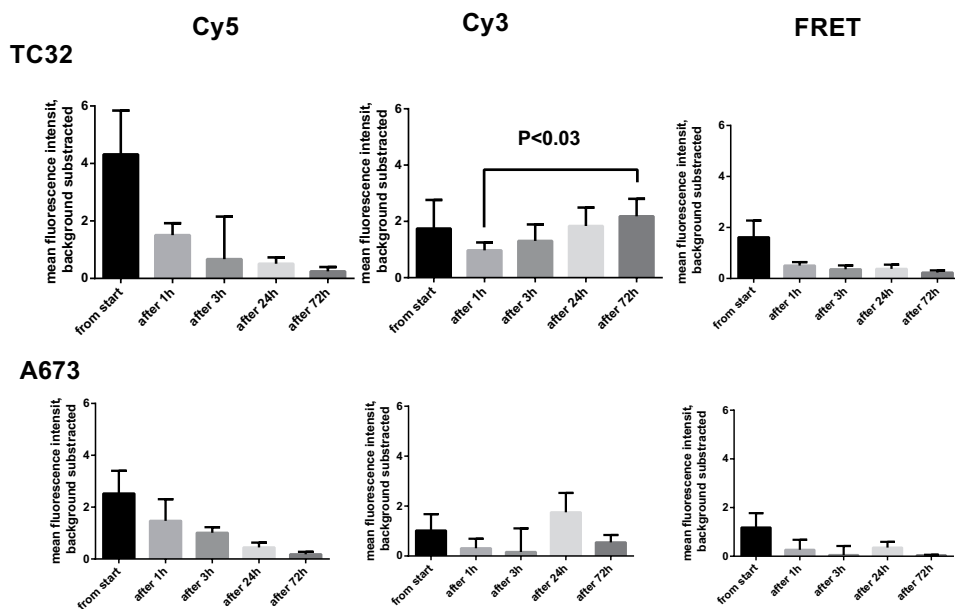


Figure 4: Mean fluorescence intensities over time in EWS cell lines TC32 and A673. After addition of Cy5-S-S-Cy3-Ac-TZ14011 confocal images of EWS cell line TC32, high *CXCR4* RNA expression, and EWS cell line A673, low *CXCR4* RNA expression, taken at five time points were analyzed with LASX software by calculating the mean fluorescence intensity. Mean with SEM of at least $n=3$ is demonstrated. A decreasing trend in Cy5 fluorescence and FRET fluorescence was observed in both cell lines. Only in TC32 an increase in Cy3 fluorescence was observed which was significant 72 h after Cy5-S-S-Cy3-Ac-TZ14011 addition compared to the Cy3 fluorescence 1 h after addition. This quantitatively validates the functionality of Cy5-S-S-Cy3-Ac-TZ14011 in a cellular environment.

DISCUSSION

Previously we demonstrated that the CXCR4 targeting peptide Ac-TZ14011-FITC was internalized over time [18]. These data, however, did not allow us to differentiate between CXCR4 that was originally residing on the surface during the labeling process and labeled-CXCR4 that might have recycled back to the surface [32,33]. This prompted us to study the live cell dynamics of CXCR4 internalization with an activatable CXCR4 endocytosis tracer (Cy5-S-S-Cy3-Ac-TZ14011) based on a disulfide-based Cy3-Cy5 FRET label linked to Ac-TZ14011. Upon cellular internalization the disulfide bond in the FRET-label was disrupted by reduction, leading to an increase in Cy3 fluorescence (**Figure 1**). Synthesis of Cy5-S-S-Cy3-Ac-TZ14011 was relatively straightforward, however solubility issues due to the charges on the dyes resulted in a low yield of the end product (**Figure 2**). The use of alternative (cyanine) dyes may improve the yield. Photophysical analyses of the unconjugated label (compound 3) demonstrated a ~95% FRET efficiency. This is consistent with expectations of FRET based on the close proximity of the two dyes ($\ll 6$ nm) compared with a R_0 distance of 6 nm reported for the Cy3-Cy5 FRET pair at which FRET efficiency is 50% [34]. The diminished increase in Cy3 signal observed when the complete tracer Cy5-S-S-Cy3-Ac-TZ14011 was reduced compared to the FRET label alone could stem from a higher initial Cy3 signal. This could be caused by minor reduction of the Cy5-S-S-Cy3-Ac-TZ14011 during coupling conditions which could not be fully removed by preparative HPLC or could be caused by leakage of the Cy3 fluorescence. The higher initial Cy3 signal was observed as well during live cell imaging at the start when a high Cy5 and FRET fluorescence of the Cy5-S-S-Cy3-Ac-TZ14011 were detected, suggesting leakage might partially be a cause (**Figure 4**). Moreover, similar FRETs earlier reported by us and others had comparable FRET efficiencies despite high purity [22,23]. During live cell evaluation of Cy5-S-S-Cy3-Ac-TZ14011, like during the synthesis, aggregates were observed but could partially be reduced by sonication of Cy5-S-S-Cy3-Ac-TZ14011 before addition to the cells. The internalization-dependent Cy3 fluorescence of Cy5-S-S-Cy3-Ac-TZ14011 shortly after internalization implies Cy5-S-S-Cy3-Ac-TZ14011 is functional and potentially suited to detect recycling of internalized CXCR4 to the cell membrane (**Figure 4, S3 and S4**). This is strengthened by the increasing trend of Cy3 signal observed in the high CXCR4 expressing EWS cell line TC32 which reached significance after 72 h compared to the Cy3 signal after 1 h. No trend in Cy3 signal was observed in the low CXCR4 expressing EWS cell line A673 [6]. This is consistent with earlier reported observation of CXCR4 expression in A673 [8]. The absence of clear membrane staining after internalization of CXCR4 and dominant overlap of Cy3 signal with the lysotracker signal suggest that in these EWS cell lines majority of the receptor is not recycled back to the membrane after internalization. However, that some receptors do relocate to the cell membrane after internalization cannot be excluded.

The principle of live cell imaging of receptor dynamics is especially for GPCRs an interesting method to study the dynamics per cell/tissue-type as without any further labeling needed and one is able to distinguish the internalized part of the studied receptor from the others. CXCR4 and other GPCRs were reported to be recycled back to the cell membrane after internalization [32,33,35]. By using Cy5-S-S-Cy3-Ac-TZ14011 it is possible to study this process. The observed absence of toxicity of Cy5-S-S-Cy3-Ac-TZ14011 might open new routes to study compound-receptor complex endocytosis. The gained insight in the CXCR4 endocytosis can be used for optimization of targeting CXCR4 in Ewing sarcoma by inhibitors which are based on Ac-TZ14011. In addition, the principle could be used to target both the CXCR4 receptor and to internalize chemotherapeutic agent carriers which can release their chemotherapeutics

in an reducing environment inside the cell which would increase their effect [36].

In conclusion, we present here a method to study live cell CXCR4 endocytosis by an activatable receptor targeting peptide Cy5-S-S-Cy3-Ac-TZ14011. Live cell evaluation in EWS cell lines confirmed the functionality of the peptide with a significant increase in Cy3 signal in a high CXCR4 expressing EWS cell line and not in a low expressing CXCR4 EWS cell line and provided insight in the cell biology of these cell lines which might lead to improved anti-CXCR4 therapy in EWS patients. The same concept may also proof to be of value for coming studies regarding (CXCR4) receptor dynamics.

ACKNOWLEDGEMENTS

This study was supported by National organization for Scientific Research (NWO) Grant NWO-TOP GO 854.10.012, by a Koningin Wilhelmina Fonds (KWF) translational research award (Grant No. PGF 2009-4344), a Netherlands Organization for Scientific Research VIDI grant (Grant No. STW BGT11272), and the 2015-2016 Post-Doctoral Molecular Imaging Scholar Program Grant granted by the Society of Nuclear Medicine and Molecular imaging (SNMMI) and the Education and Research Foundation for Nuclear Medicine and Molecular Imaging.

REFERENCES

- 1 Nagasawa, T. CXCL12/SDF-1 and CXCR4. *Front Immunol* **6**, 301, (2015).
- 2 Guo, F. *et al.* CXCL12/CXCR4: a symbiotic bridge linking cancer cells and their stromal neighbors in oncogenic communication networks. *Oncogene*, (2015).
- 3 Lippitz, B. E. Cytokine patterns in patients with cancer: a systematic review. *Lancet Oncol* **14**, e218-e28, (2013).
- 4 Sand, L. G. L., Szuhai, K. & Hogendoorn, P. C. W. Sequencing overview of Ewing sarcoma: a journey across genomic, epigenomic and transcriptomic landscapes. *Int J Mol Sci* **16**, 16176-215, (2015).
- 5 De Alava, E., Lessnick, S. L. & Sorensen, P. H. in *WHO Classification of Tumors of Soft Tissue and Bone* (eds C.D.M. Fletcher, J.A. Bridge, P. C. W. Hogendoorn, & F. Mertens) 306-9 (IARC, 2013).
- 6 Sand, L. G. L. *et al.* CXCL14, CXCR7 expression and CXCR4 splice variant ratio associate with survival and metastases in Ewing sarcoma patients *Eur J Cancer*, (2015).
- 7 Bennani-Baiti, I. M. *et al.* Intercohort Gene Expression Co-Analysis Reveals Chemokine Receptors as Prognostic Indicators in Ewing's sarcoma. *Clin Cancer Res* **16**, 3769-78, (2010).
- 8 Krook, M. A. *et al.* Stress-Induced CXCR4 Promotes Migration and Invasion of Ewing sarcoma. *Mol Cancer Res* **12**, 953-64, (2014).
- 9 Reddy, K. *et al.* Stromal cell-derived factor-1 stimulates vasculogenesis and enhances Ewing's sarcoma tumor growth in the absence of vascular endothelial growth factor. *Int J Cancer* **123**, 831-7, (2008).
- 10 Pelekanos, R. A. *et al.* Intracellular trafficking and endocytosis of CXCR4 in fetal mesenchymal stem/stromal cells. *BMC Cell Biol* **15**, 15-, (2014).
- 11 Marchese, A. Endocytic trafficking of chemokine receptors. *Curr Opin Cell Biol* **27**, 72-7, (2014).
- 12 Cepeda, E. B. *et al.* Mechanisms regulating cell membrane localization of the chemokine receptor CXCR4 in human hepatocarcinoma cells. *BBA-Mol Cell Res* **1853**, 1205-18, (2015).
- 13 Busillo, J. M. & Benovic, J. L. Regulation of CXCR4 Signaling. *Biochim Biophys Acta* **1768**, 952-63, (2007).
- 14 van Buul, J. D. *et al.* Leukocyte-Endothelium Interaction Promotes SDF-1-dependent Polarization of CXCR4. *J Biol Chem* **278**, 30302-10, (2003).
- 15 Orsini, M. J., Parent, J.-L., Mundell, S. J. & Benovic, J. L. Trafficking of the HIV coreceptor CXCR4: role of arrestins and identification of residues in the c-terminal tail that mediate receptor internalization. *J Biol Chem* **274**, 31076-86, (1999).
- 16 Kuil, J., Buckle, T. & van Leeuwen, F. W. B. Imaging agents for the chemokine receptor 4 (CXCR4). *Chem Soc Rev* **41**, 5239-61, (2012).
- 17 Kuil, J., Velders, A. H. & van Leeuwen, F. W. B. Multimodal tumor-targeting peptides functionalized with Both a Radio- and a Fluorescent Label. *Bioconjug Chem* **21**, 1709-19, (2010).
- 18 van den Berg, N. S., Buckle, T., Kuil, J., Wesseling, J. & van Leeuwen, F. W. B. Immunohistochemical

- Detection of the CXCR4 Expression in Tumor Tissue Using the Fluorescent Peptide Antagonist Ac-TZ14011-FITC. *Transl Oncol* **4**, 234-40, (2011).
- 19 Buckle, T. *et al.* Use of a Single Hybrid imaging agent for integration of target validation with *in vivo* and
ex vivo imaging of mouse tumor lesions resembling human DCIS. *PLoS One* **8**, e48324, (2013).
- 20 Ni, Q., Titov, D. V. & Zhang, J. Analyzing protein kinase dynamics in living cells with FRET reporters.
Methods **40**, 279-86, (2006).
- 21 Urano, Y. Novel live imaging techniques of cellular functions and *in vivo* tumors based on precise design
of small molecule-based 'Activatable' fluorescence probes. *Curr Opin Chem Biol* **16**, 602-8, (2012).
- 22 Rood, M. T. M. *et al.* An activatable, polarity dependent, dual-luminescent imaging agent with a long
luminescence lifetime. *Chemical Communications* **50**, 9733-6, (2014).
- 23 Yang, J., Chen, H., Vlahov, I. R., Cheng, J.-X. & Low, P. S. Evaluation of disulfide reduction during recep-
tor-mediated endocytosis by using FRET imaging. *Proceedings of the National Academy of Sciences* **103**,
13872-7, (2006).
- 24 Roy, R., Hohng, S. & Ha, T. A practical guide to single-molecule FRET. *Nat Meth* **5**, 507-16, (2008).
- 25 Iqbal, A. *et al.* Orientation dependence in fluorescent energy transfer between Cy3 and Cy5 terminally
attached to double-stranded nucleic acids. *Proceedings of the National Academy of Sciences* **105**, 11176-81,
(2008).
- 26 KleinJan, G. *et al.* Fluorescent Lectins for Local *in Vivo* Visualization of Peripheral Nerves. *Molecules* **19**,
9876, (2014).
- 27 Spa, S. J. *et al.* Orthogonal Functionalization of Ferritin via Supramolecular Re-Assembly. *Eur J Inorg*
Chem, n/a-n/a, (2015).
- 28 Patterson, S. D. & Katta, V. Prompt Fragmentation of Disulfide-Linked Peptides during Matrix-Assisted
Laser Desorption Ionization Mass Spectrometry. *Anal Chem* **66**, 3727-32, (1994).
- 29 Hanaoka, H. *et al.* Development of a ¹¹¹In-labeled peptide derivative targeting a chemokine receptor,
CXCR4, for imaging tumors. *Nucl Med Biol* **33**, 489-94, (2006).
- 30 Mujumdar, R. B., Ernst, L. A., Mujumdar, S. R., Lewis, C. J. & Waggoner, A. S. Cyanine dye labeling re-
agents: Sulfoindocyanine succinimidyl esters. *Bioconjug Chem* **4**, 105-11, (1993).
- 31 Ottaviano, L. *et al.* Molecular characterization of commonly used cell lines for bone tumor research: A
trans-European EuroBoNet effort. *Genes Chromosomes Cancer* **49**, 40-51, (2010).
- 32 Förster, R. *et al.* Intracellular and Surface Expression of the HIV-1 Coreceptor CXCR4/Fusin on Various
Leukocyte Subsets: Rapid Internalization and Recycling Upon Activation. *The Journal of Immunology*
160, 1522-31, (1998).
- 33 Patrussi, L. *et al.* Enhanced Chemokine Receptor Recycling and Impaired S1P1 Expression Promote Leu-
kemic Cell Infiltration of Lymph Nodes in Chronic Lymphocytic Leukemia. *Cancer Res* **75**, 4153-63,
(2015).
- 34 Ha, T. *et al.* Initiation and re-initiation of DNA unwinding by the Escherichia coli Rep helicase. *Nature*
419, 638-41, (2002).
- 35 David, R. Endocytosis: Sorting the recycling. *Nat Rev Mol Cell Biol* **12**, 3-, (2011).
- 36 Mei, L. *et al.* Enhanced antitumor and anti-metastasis efficiency via combined treatment with CXCR4
antagonist and liposomal doxorubicin. *J Control Release* **196**, 324-31, (2014).

SUPPLEMENTARY FIGURES

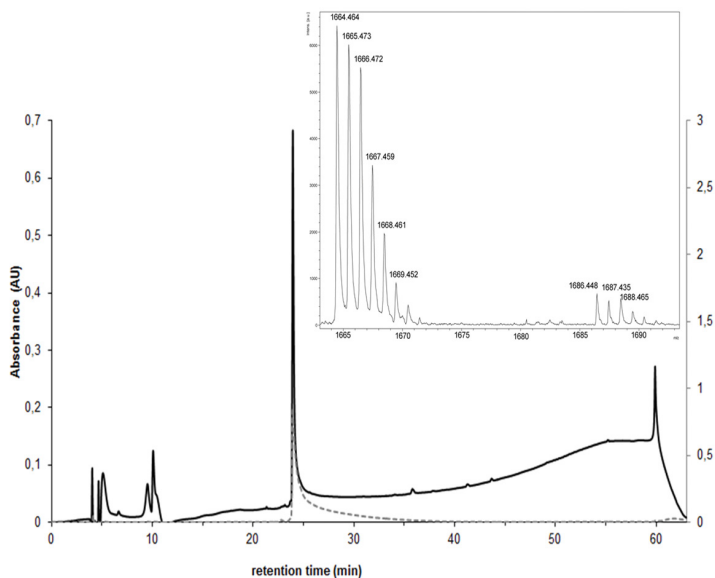


Figure S1: HPLC trace with inset MALDI-TOF of compound 3 injected in PBS with 220 nm absorbance in black and 650 nm absorbance in grey. A mass of 1664.46 Da was measured for compound 3 which is corresponding to the calculated mass of 1685.41 Da.

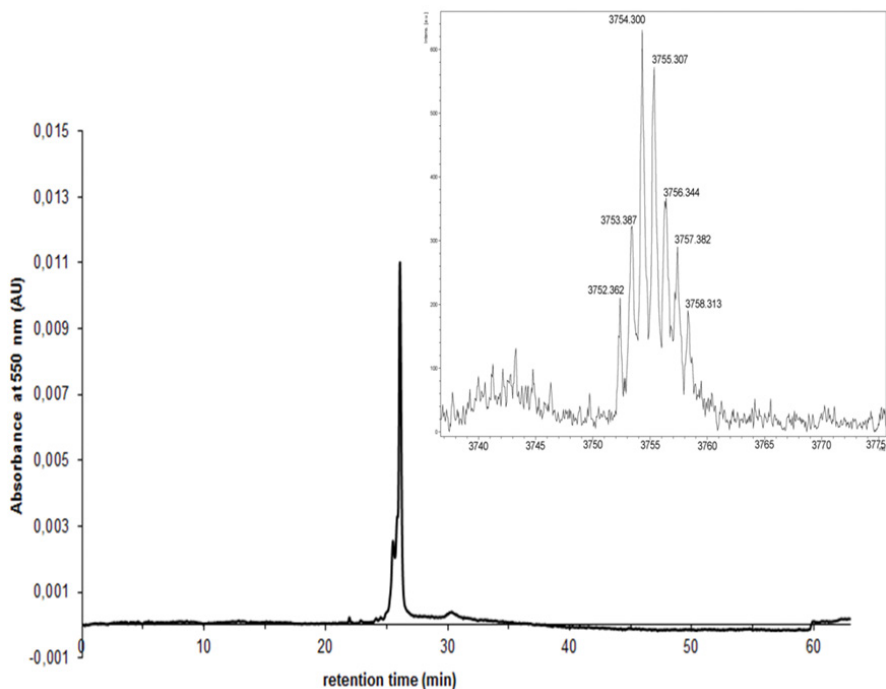


Figure S2: HPLC trace with inset MALDI-TOF of compound 4 (*Cy-S-S-Cy3-Ac-TZ14011*) injected in PBS. The measured mass of *Cy-S-S-Cy3-Ac-TZ14011* was 3752.36 Da which was corresponding to the calculated mass of 3751.49 Da

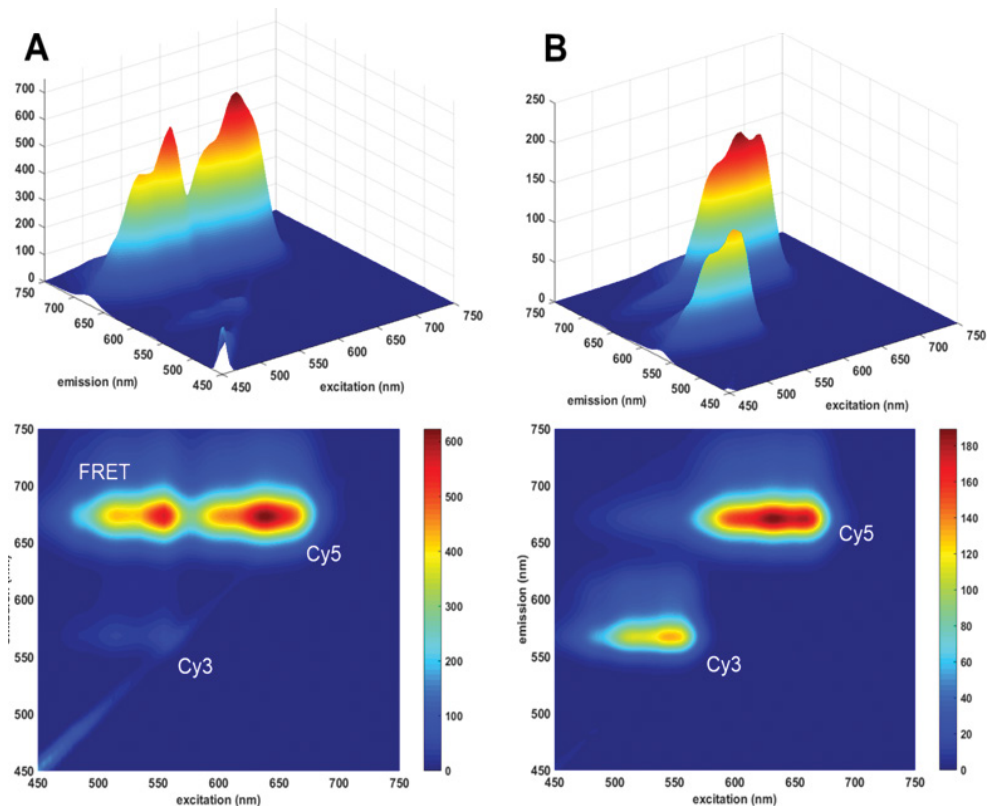
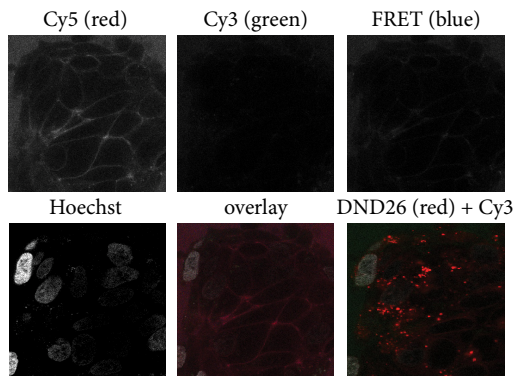


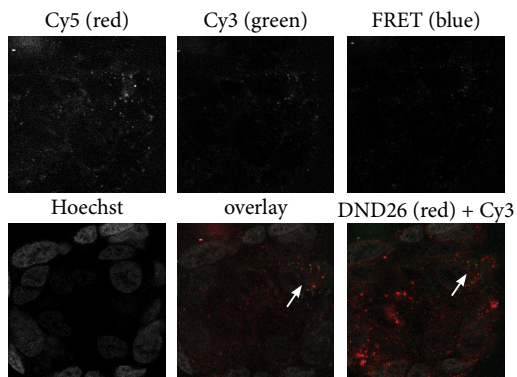
Figure S5: 2D and 3D representation of the excitation/emission spectrum of compound 3 ($3\mu\text{M}$ in PBS) prior to (A) and after DTT incubation (B) 140min. The photophysical properties of compound 3 (Cy5-S-S-Cy3) were determined by spectrofluorometry. **A**) Prior to reduction of the disulfide bond, compound 3 showed high FRET fluorescence (excitation between 500-570 nm and emission between 650-700 nm) and some Cy3 fluorescence (excitation between 500-570 nm and emission between 550-600 nm). **B**) After reduction of the disulfide bond by DTT the FRET fluorescence was almost completely reduced and the Cy3 fluorescence was highly increased. This demonstrates the in vitro functionality of compound 3 and its emission specificity. The gain of the spectrometer was reduced in the spectrum B to avoid oversaturation.

Figure S4 TC32

A: from start



B: after 1 h



C: after 3 h

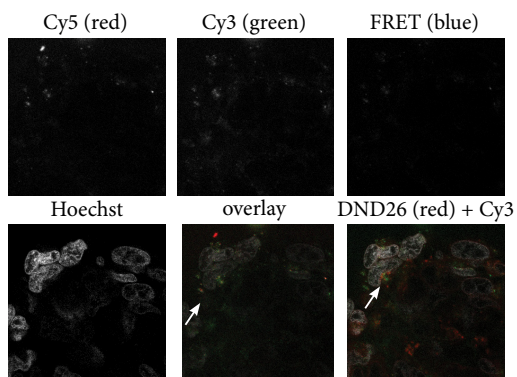
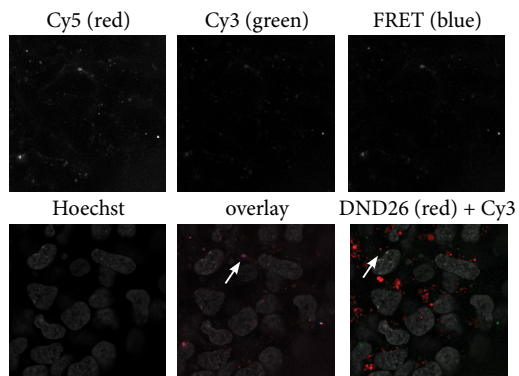
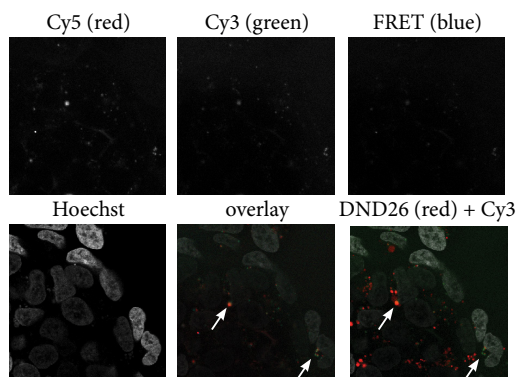


Figure S5 A673

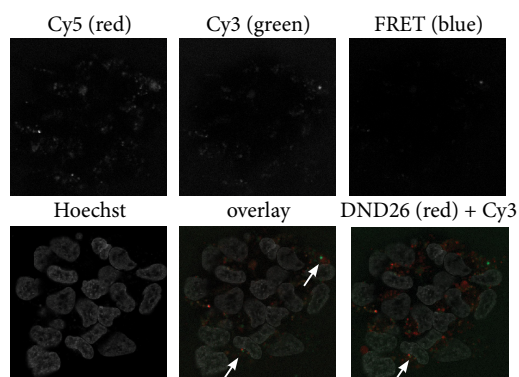
A: from start



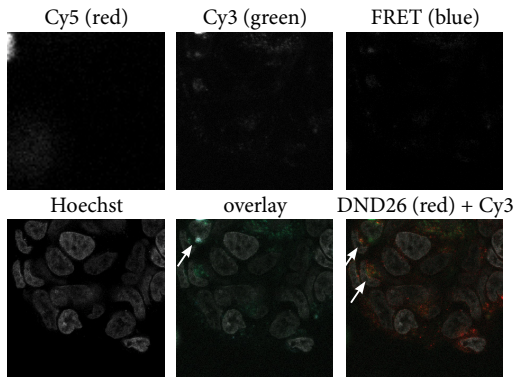
B: after 1 h



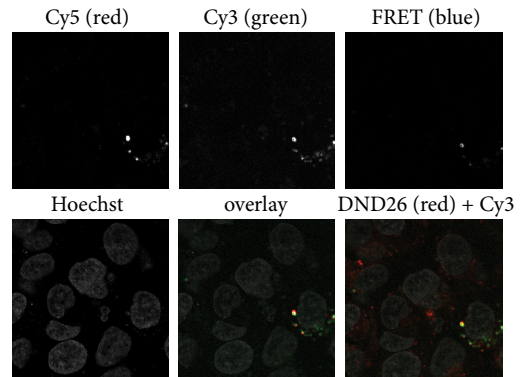
C: after 3 h



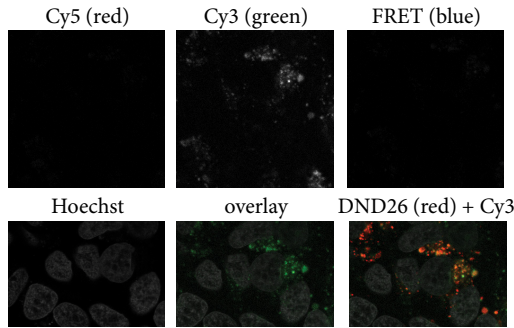
D: after 24 h



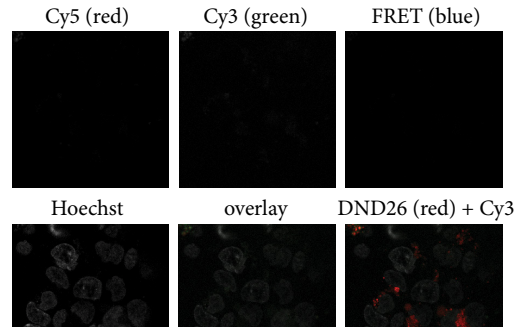
D: after 24 h



E: after 72 h



E: after 72 h



Supplementary description Figure S3 and S4: Representative images ($n > 3$) were collected during live cell imaging of high CXCR4 expressing EWS cell line TC32 (S4) and low CXCR4 expressing EWS cell line A673 (S5). Hoechst, lysotracker DND-26 and the Cy5, FRET, Cy3 signals emitted by Cy-S-S-Cy3-Ac-TZ14011 were excited, and emission was detected at the wavelengths described in **Table 1**. Color labels of the signals in the overlay are stated brackets. After addition of Cy-S-S-Cy3-Ac-TZ14011 a cell membrane staining pattern was shown in TC32 by the Cy5 and FRET signals (S4a). In A673 this was less pronounced (S5a). No Cy3 signal was observed in TC32 and only at a few sites in A673 (arrow). After 1 h, especially in TC32, the Cy5 signal was more clustered (S4b and S5b). Internalized peptide is observed in both cell lines, indicated by the overlap with the DND26 signal (arrow at DND26 + Cy3). This overlap is present throughout the rest of the imaging process and was most present after 72 h in TC32. Overlap of all three the peptide emitted signals is demonstrated at some sites (arrows in overlays). This overlap suggests a combination of reduced and non-reduced of Cy-S-S-Cy3-Ac-TZ14011 at the same position. Overall decrease of Cy5 and the FRET signals over time was observed in both TC32 and A673 and was almost absent at 72 h. Increase of Cy3 signal over time could only be observed in TC32. This implies that Cy-S-S-Cy3-Ac-TZ14011 is functional in an cellular environment and that the CXCR4 bound by Cy-S-S-Cy3-Ac-TZ14011 is directed to the lysosomes in TC32 upon internalization over a time course of at least 72 h.

